FISEVIER

Contents lists available at ScienceDirect

Science of the Total Environment

journal homepage: www.elsevier.com/locate/scitotenv



Investigation of the biochemical controls on mercury uptake and mobility in trees



Mae Sexauer Gustin ^{a,*}, Sarrah M. Dunham-Cheatham ^a, Jeffrey F. Harper ^b, Won-Gyu Choi ^b, Joel D. Blum ^c, Marcus W. Johnson ^c

- ^a Department of Natural Resources & Environmental Science, University of Nevada, Reno, 1664 N. Virginia Street, Mail Stop 186, Reno, NV 89557, USA
- ^b Department of Biochemistry & Molecular Biology, University of Nevada, Reno, Reno, NV 89557, USA
- ^c Department of Earth and Environmental Science, University of Michigan, 1100 N University, Ann Arbor, MI 48109, USA

HIGHLIGHTS

- Aspen and Austrian pine were subjected to spikes of gaseous Hg(0); MeHg via the roots.
- After the spike, aspen moved spiked Hg (0) into new growth; MeHg had no impact.
- Aspen resorbed foliar Hg in the fall; pine did not.
- Aspen foliage had Hg concentrated in the cell wall and not associated with sulfur.
- Results explain why aspen tree rings are not suitable archives for atmospheric Hg.

GRAPHICAL ABSTRACT



ARTICLE INFO

Editor: Jay Gan

Keywords:
Foliar partitioning
Mercury isotopes
Methylmercury
Pinus nigra
Populus tremuloides

ABSTRACT

Atmospheric elemental mercury (Hg(0)) enters plant stomata, becomes oxidized, and is then transferred to annual growth rings providing an archive of air Hg(0) concentrations. To better understand the processes of Hg accumulation and translocation, the foliage of quaking aspen and Austrian pine were exposed to Hg(0), and methylmercury (MeHg) or Me^{198} Hg via roots, in controlled exposures during the summer. Isotopic measurements demonstrated, in a laboratory setting, that the natural mass-dependent fractionation observed was the same as that measured in field studies, with the lighter isotopes being preferentially taken up by the leaves. Hg was measured in plant tissues across seasons. Aspen trees moved Hg into new growth immediately after exposure, resorbed Hg in the fall, and then distributed Hg to new growth tissues in the spring. Austrian pine did not reallocate Hg. Mercury measured in aspen leaf fractions of trees exposed to Hg(0) demonstrated that 85 % of Hg was in the cell wall. It was also found that redox-active molecules, such as H_2O_2 , could potentiate the release of cell wall-bound Hg from aspen leaves, providing a potential mechanism for remobilization. Regardless of the mechanism, the ability of aspen to reallocate Hg to new tissues indicates that Hg distribution in tree rings from aspen do not provide a reliable record of yearly changes in atmospheric Hg(0).

1. Introduction

The role of plants in the mercury (Hg) biogeochemical cycle came under scrutiny in the 1990's with the realization that litterfall was a significant source of Hg to soils. It was proposed that the source of Hg in litterfall

^{*} Corresponding author.

E-mail address: mgustin@unr.edu (M.S. Gustin).

could be elemental Hg uptake via the stomata, uptake from soil, or foliage surface oxidation of elemental Hg to water-soluble forms that were washed off to the soil with precipitation (Munthe et al., 1995; Iverfeldt, 1991). It is now known that plants primarily take up gaseous elemental Hg (Hg(0)) via stomata and Hg is accumulated in foliage. In the leaf, Hg(0) is oxidized and transported to tree rings where Hg is stored, and some tree species provide an archive of atmosphere Hg(0) concentrations. It is not yet clear where Hg (0) gets oxidized inside the foliage. It is possible that Hg is assimilated into metabolically active cells, or remains outside the cell, and is oxidized via redox reactions (Dixon and Barros, 2019) that occur in cell walls. Regardless, further movement has been proposed to occur as cysteine adducts (Dennis et al., 2019; Manceau et al., 2019), eventually moving through the phloem into growth rings (Arnold et al., 2018).

Ericksen et al. (2003) described the use of large mesocosms and aspen growing in soils amended with Hg-contaminated mill tailings (12.3 \pm 1.3 μg Hg g $^{-1}$) and those grown in "clean" soil (0.03 \pm 0.01 μg Hg g $^{-1}$) to understand the exchange of Hg between plants and the atmosphere. Results demonstrated that plant foliage was primarily a sink for atmospheric Hg and plants did not move Hg from the soil to the air. MeHg concentrations represented $\sim\!1$ % of the total Hg (HgT) observed in foliage, consistent with typical leaf MeHg concentrations of <5 % of HgT (Liu et al., 2021). Arnold et al. (2018) and Peckham et al. (2019a, 2019b), using Austrian pine and root spikes of HgBr₂, also found this did not result in any significant effect on HgT in foliage or tree rings. A lack of an effect of Hg addition to roots has also been demonstrated for HgCl₂ (c.f., Millhollen et al., 2006; Stamenkovic and Gustin, 2009; Ericksen and Gustin, 2004).

In other controlled experiments using 4 y old aspen and Austrian pine trees, Arnold et al. (2018) found air Hg(0) concentrations had a significant effect on foliar concentrations and tree ring concentrations. Peckham et al. (2019a, 2019b) demonstrated that Austrian pine translocated Hg via the stomata to the tree rings, and this was affected by local environmental conditions. They concluded that trees are active samplers of Hg and that leaf area influences observed tree ring concentrations. Peckham et al. (2019a, 2019b) hypothesized, based on limited data, that resorption of Hg from needles of Austrian pine occurred in the fall.

Hg complexes in foliage are typically thought to be associated with reduced sulfur compounds, such as cysteine, glutathione, and phytochelatins, or as mercury sulfide nanoparticles (Manceau et al., 2019; Carrasco-Gil et al., 2013). The plant cell wall itself is a site for many redox reactions, such as in lignin biosynthesis (Dixon and Barros, 2019). It has been proposed that Hg oxidation in foliage occurs through interaction with reactive oxygen species that are generated during photosynthesis and respiration (Liu et al., 2021). In foliage, the catalase enzyme catalyzes hydroperoxide decomposition at a rate constant of $10^7~{\rm M~s^{-1}}$ (Tehrani and Moosavi-Movahedi, 2018; Vainshtein et al., 1981). Du and Fang (1983) found through in vivo and in vitro experiments that Hg accumulation in foliar tissue was proportional to catalase activities. Higher catalase activity points toward tissues with higher rates of hydrogen peroxide (H₂O₂) oxidation that could convert Hg(0) into oxygen-bound adducts or make Hg(II) available so it can bind with sulfur-based and other compounds.

The use of natural abundance Hg isotopes to trace Hg sources and biochemical processes in organisms and plants provides important information; however, data must be interpreted with the knowledge that Hg isotopes can fractionate during chemical reactions involving Hg or via photochemical processes. For example, Demers et al. (2013) investigated Hg cycling in a 10 y old aspen stand at a Free Air Carbon Experiment (FACE) site in Wisconsin, USA, and found that plants preferentially assimilated the light isotopes of Hg. Similarly, Wang et al. (2021) measured Hg isotopes in tree rings of Masson pine (*Pinus massoniana*) and found mass-dependent fractionation (MDF) and a slight change in odd numbered isotope massindependent fractionation (odd-MIF) due to reductive loss of Hg associated with foliage. Using Hg isotopes, Yuan et al. (2019) demonstrated that reemission of Hg(0) occurred after reductive loss from evergreen foliage surfaces and the interior of leaves. Odd-MIF was associated with foliage and linked to foliar release from Hg-S compounds, with 70 % from the leaf

interior and 30 % from the leaf surface. Finally, Kurz et al. (2020) demonstrated that isotope fractionation during foliar uptake resulted in diel variation in the mass-dependent and mass-independent isotopic composition of gaseous Hg(0) in forests.

Here we investigated how a high dose of Hg(0) was partitioned in aspen and Austrian pine, and the potential for reallocation after exposure. In addition, the location where foliar Hg is sequestered was investigated along with potential mechanisms for remobilization. Experiments were conducted with the goal of tracking the movement of Hg spikes in the trees across seasons. Tree tissues were divided by type, age, and growth (pre-, during, or post-Hg exposure) and quantified for HgT concentrations. MeHg was quantified in select tissues for both tree types. For aspen, Hg isotope ratios in homogenized foliage were measured, and Hg concentrations were measured in 3 separate foliage components (i.e., cell wall, membranes, and soluble fractions). Based on the results of the latter, the hypothesis that Hg bound to the foliage cell wall can be readily dissociated by reactive oxygen compounds generated by enzymes (e.g., superoxide dismutases, and/or NADPH-dependent oxidases, such as RBOHs) located in the plant cell plasma membrane and apoplast was tested. If this hypothesis is correct, it provides a potential pathway during senescence by which cell wall-bound Hg could be remobilized and transported to other tissues (Mhamdi and Van Breusegem, 2018). Finally, this study also allowed us to test the hypothesis of Peckham et al. (2019a, 2019b) that Austrian pine trees resorb Hg during senescence.

2. Methods

2.1. Aspen

2.1.1. Experimental design & exposures

One y old (n=80) aspen trees were purchased from Rail City Garden Center (Reno, Nevada, USA) and moved to a greenhouse bay at the University of Nevada, Reno (UNR) Valley Road Greenhouse Complex (VR) on May 20, 2019. Trees were randomly divided into one of 4 groups: 1) air exposure to Hg(0); 2) root spike of MeHg; 3) root spike of isotopically enriched Me¹⁹⁸Hg; and 4) control. The control group was exposed to the same growth conditions as the 3 treatment groups. Five trees were harvested before the start of the experiment to determine the initial "pre-exposure" Hg concentration in the tissues and soil.

The exposure of trees to treatments occurred over 17 days in July 2019, and was accomplished by placing each group of trees into separate growth chambers. For a detailed description of the handling and preparation of trees and the construction of the exposure chambers, see the Supplemental Information (SI). Hg(0) was diffused into one treatment chamber (see SI) from a bead of elemental Hg held in an air-tight polytetrafluoroethylene bottle at 25 °C in a refrigerated bath. A polyfluoroalkyl valve was placed in-line between the Hg source and the chamber inlet. A pulse of Hg (0) vapor was added to the chamber by opening the valve until the Hg (0) concentration reached 500 ng m $^{-3}$, then closing the valve and allowing the concentration to decay. MeHg and Me 198 Hg treatments received a total of 0.3 μg Hg as MeHg. Stock solutions, prepared in Type I water, were made using MeHg (Brooks Rand, P/N 06610) for the MeHg treatment and isotopically enriched ¹⁹⁸Hg methylmercury (National Research Council of Canada, P/N EMMS-1) for the Me¹⁹⁸Hg treatment. One 10 mL aliquot of the stock solution was added weekly by pipette to the moist soil 15 cm deep and 5 cm horizontal distance from the tree bole, with each addition added to a different location in the pot to avoid overdosing one area of the root mass.

HgT air concentrations in each treatment chamber, along with the greenhouse bay, were measured using a Tekran® 2537 Hg analyzer at a 5 min resolution; chambers were sampled in rotation by the single analyzer. Concentrations in the exposure chamber ranged between $\sim\!300$ to 1000 ng Hg m $^{-3}$ over the course of a day, with concentrations highest after the spike addition and lowest at night. Hg(0) concentrations were 1.95 \pm 1.25 ng Hg m $^{-3}$ in the greenhouse bay. Temperature (T) and relative humidity (RH) were recorded every 5 min with a Campbell Scientific

CR10X datalogger equipped with 2 probes (Campbell Scientific, P/N HMP45C), one for continuously monitoring the greenhouse bay, and one rotated between the chambers. Bay and chamber relative humidity ranged from 20 to 80 %, with the highest values during the night. Temperature for the bay ranged between 17.5 and 27 $^{\circ}$ C from night to day, respectively, with the chambers being hotter than the bay by 7 to 10 $^{\circ}$ C. After the exposure was completed, the trees were removed from the growth chambers and randomized in the greenhouse, mixing the different treatments.

A small dot of nail polish was added to each leaf near the petiole to aid in partitioning foliage into groups and foliage types, using different colors; the Hg mass added was negligible, with <0.05 ng Hg added per dot. Marked foliage included: 1) pre-exposure old foliage (Pre-old), that extended from the bole up to 15.25 cm along each branch, and from the bottom of the tree to 30.5 cm from the top of the bole; 2) pre-exposure new foliage (Pre-new), or foliage on each branch that was over 15.25 cm from the bole and along the top 30.5 cm of the bole; 3) foliage that emerged during the 17-day exposure (During); and 4) new foliage (Post), that emerged after the end of the exposures, and During foliage was marked upon removal of trees from the growth chambers.

2.1.2. Tree harvesting

Six trees from each group (n = 24 total) were harvested 18 days after the completion of the exposures. The duration between exposure and harvest was permitted to provide time for the trees to process the Hg under more optimal growing conditions (i.e., outside of the growing chambers). Two aliquots of soil were collected and bulked from each pot using a 2.5 cm diameter soil auger to sample soil from the entire pot depth. The auger was rinsed with Type I water and dried between each pot. Root masses were extracted from the soil and separated from the tree bole using an ethanol-cleaned pruner. The roots were then rinsed with copious amounts of Type I water until the rinse water was clear and no more soil could be removed. Branches and foliage were removed from the tree bole, and the bole segmented into 10 cm segments, starting at the base of the bole and working toward the top. Denuded branches were collected separately. Foliage was divided into one of the 4 foliage types (i.e., Preold, Pre-new, During, and Post) based on the color of the paint dot on each leaf. Once a tissue was removed from the tree, it was placed in a new, sterile 50 mL conical tube or a new double Ziploc freezer bag and placed in a 20 °C freezer. An aliquot of each tissue type was placed in separate storage containers and immediately frozen with liquid nitrogen and stored at -80 °C; these samples were used for the foliage fractionation analyses, described below.

Replicate trees (n=3–4) from each group were moved outside and planted in the ground directly adjacent to the bay. The soil at this location is a fine-loamy, mixed, superactive, mesic Aridic Argixeroll. Once planted, the trees were watered 2–3 times each week until the first frost. Foliage was collected from these trees in the autumn as the foliage was senescing to assess if the trees removed Hg from the foliage in preparation for winter (e.g., is Hg in foliage mobile?).

2.2. Austrian pine

2.2.1. Experimental design & exposures

Three y old Austrian pine trees (n=35) were purchased from the Washoe County Tree Nursery on June 3, 2020, and placed in the UNR Environmental Research Facility (ERF) greenhouse (c.f., Arnold et al., 2018); twenty trees were placed in bay 1 and 15 trees in bay 2. After 9 days of acclimation, 5 trees from bay 1 were harvested as initial controls. Trees in bay 2 were simultaneously dosed with Me¹⁹⁸Hg via the roots and Hg(0) exposure to the aerial tissues. Trees in bay 1 were not exposed to Hg. Exposures lasted for 3 weeks, and then 5 trees were harvested from bays 1 and 2. The remaining trees (n=20) were moved to VR and planted outside. Five control and 5 treated trees were harvested in September 2020 and another set of 5 trees per group were harvested in late May 2021. Twist ties of different colors were added to branches to delineate foliage

categories, including: "Pre", bole and needle growth from the third year growth (2020); "During", obvious new growth that occurred during the 3-week exposure, if any; and "Post", bole and needle growth that occurred after overwintering outside during the 2020–2021 winter season.

Gaseous Hg(0) concentrations, T, and RH of each bay were continuously monitored for the duration of the exposures. Gaseous Hg(0) concentrations were measured by a Tekran® 2537A at 2.5 min resolution, switching between bay 1 and bay 2 every 3 cycles (7.5 min in each bay). Hg(0) was permeated into bay 2 at a concentration of 100 to 200 ng Hg m $^{-3}$ for $\sim\!60$ s. This was achieved by pumping ambient air from the ERF head house across a Hg(0) permeation tube held at 10 °C in a refrigerated water bath and into bay 2. Temperature and RH were measured at 5 min resolution using a Campbell Scientific CR100 equipped with 2 sensors, one placed in each bay. RH ranged from 10 to 40 %, with nighttime values being larger; T ranged from 10 to 40 °C in bay 1, and for bay 2 temperatures were the same as bay 1 overnight but 5 °C higher during the day. Trees were watered every 2–3 days during the exposure and once they were planted outside (until the first frost).

2.2.2. Tree harvesting

Trees and soil were harvested similarly to the aspen trees above. Needles were individually removed from the bole and branches and divided into Pre, During, and Post, and 2021 needle groups based on the twist tie delineations. Denuded branches and boles were cut at the twist ties and divided into Pre, During, and Post, and 2021 bole groups. Once a sample was removed from the tree, it was placed in a new, sterile 50 mL conical tube or a new double Ziploc freezer bag and placed in a $-20\,^{\circ}\text{C}$ freezer.

2.3. Analytical methods

2.3.1. Total Hg analysis

Aliquots of tree tissues for HgT analysis were lyophilized using a Harvest Right freeze dryer with a 5.25 h freeze and 16 h dry cycle. Lyophilized tissues were stored in air-tight containers at $-20\,^{\circ}\mathrm{C}$ until analyzed. Dried tissues were homogenized using an ethanol-cleaned spatula to grind and powder the material. Triplicate aliquots of each homogenized sample were analyzed for HgT concentrations using a direct Hg analyzer (EPA Method 7473; Milestone DMA-80 evo tri-cell). Aqueous standards were used to calibrate the instrument following standard methods; certified reference materials (CRMs; NIST) were used to validate instrument accuracy ($\pm\,10\,$ %) and precision (RSD $<\,5\,$ %) at the beginning of each analytical batch, and ongoing check standards were analyzed within every 10 samples.

2.3.2. Methylmercury analysis

MeHg concentrations were quantified following EPA Method 1630 (detection limit 0.02 ng g $^{-1}$). Briefly, small aliquots (0.10 g) of dried, homogenized tissue were digested in 10 mL 25 % potassium hydroxide in methanol solution at 90 °C for 6 h, chilled, then diluted to 30 mL with methanol and swirled to homogenize. A 100 μL aliquot of the digestate was added to acetate buffer at pH 4.5 and ethylated using sodium tetraethylborate (Strem Chemicals). Samples were quantified using a Tekran 2700 automated methylmercury analysis system. Aqueous standards (Brooks Rand) and CRMs (DORM-4) were used to calibrate and validate the instrument performance and verify the digestion efficiency (± 10 %).

2.3.3. Foliage tissue component separation

Foliar tissue from aspen trees harvested after the exposure were separated into cell wall, membranes, and soluble fractions (n=13 trees, 47 samples). The fractions were analyzed for HgT concentrations following the method above. For complete tissue separation method details, see the SI.

2.3.4. H₂O₂ analyses

To test for the potential effect of $\rm H_2O_2$ mobilization of Hg from foliage cell walls during senescence, foliage cell walls were isolated in the presence

of H_2O_2 in a tissue homogenization buffer. For details of this experiment, see the SI.

2.3.5. Sulfur analyses

Foliage tissues were homogenized and the sulfur contents were quantified in crude homogenates and a purified cell wall fraction using an ICP-MS (Shimadzu 2030, University of Nevada, Reno Core Analytical Laboratory; detection limit 0.1 μ g L⁻¹). To calculate the concentration, method blanks were subtracted from the sample concentration in units of μ g L⁻¹. The concentration was then multiplied by the total extraction volume and then divided by the sample mass (total 0.014 g fresh weight of tissue in digested sample) to get the concentration in μ g g⁻¹.

2.3.6. Isotopic analysis

Hg isotope ratios were measured with high precision so that we could monitor both natural isotope fractionation of natural abundance Hg (0) and MeHg, and measure small additions of an enriched $\mathrm{Me}^{198}\mathrm{Hg}$ tracer added to soil. Hg was purified for isotopic analysis from plant tissues by dual-stage combustion and trapping followed by purge-and-trap sample matrix removal (Biswas et al., 2008). Slow controlled combustion, described by Demers et al. (2013), was applied. In-line trapping was done in an oxidizing solution of 1 % KMnO₄ (w/w) in 10 % sulfuric acid. Sample solutions were analyzed for Hg isotopic composition at the University of Michigan by cold vapor, multi-collector, inductively coupled plasma mass spectrometry using a Nu-Plasma instrument. A thallium internal spike and sample standard bracketing were used for instrumental mass bias correction (Blum et al., 2014).

MDF is defined as:

$$\delta^{202} Hg = \left\{ \left[\left(^{202} Hg/^{198} Hg\right)_{sample} \div \left(^{202} Hg/^{198} Hg\right)_{NIST~3133} \right] - 1 \right\} \tag{1}$$

While MIF is as follows:

$$\Delta^{199} Hg = \delta^{199} Hg_{measured} - \left(\delta^{202} Hg_{measured} \times 0.2520\right) \tag{2} \label{eq:delta_scale}$$

$$\Delta^{200} Hg = \delta^{200} Hg_{measured} - \left(\delta^{202} Hg_{measured} \times 0.5024\right) \tag{3}$$

$$\Delta^{201}Hg = \delta^{201}Hg_{measured} - \left(\delta^{202}Hg_{measured} \times 0.7520\right) \tag{4} \label{eq:delta_delt$$

$$\Delta^{204}Hg = \delta^{204}Hg_{measured} - \left(\delta^{202}Hg_{measured} \times 1.493\right) \tag{5} \label{eq:delta_scale}$$

For details on the Hg isotope analyses, see the SI.

2.4. Data analysis

Statistical analyses, that included t-tests, were performed using Microsoft Excel.

3. Results & discussion

3.1. *Aspen*

3.1.1. Distribution of Hg in aspen

Hg concentrations of foliage on the aspen trees that were subjected to MeHg exposures via the soil were not significantly different from the control (t-tests with equal and unequal variances, with p values ranging from 0.16 to 0.34 and only one being <0.1 (control vs. Me¹⁹⁸Hg Pre-old foliage, p=0.08)). Root concentrations of the MeHg exposures were not significantly different than for the control or pre-exposure trees. Soil, stem, and branches HgT concentrations were not significantly different between the MeHg exposures and the controls.

In contrast, after the Hg(0) exposure, foliage that was already present on the trees prior to exposure had very high Hg concentrations (Pre-old: $1702 \pm 237 \text{ ng Hg g}^{-1}$ and Pre-new: $1774 \pm 210 \text{ ng Hg g}^{-1}$; Table 1), compared to foliage that grew during the treatment (During: 531 ± 115 ng Hg g⁻¹). Foliage that grew after the treatment (Post) had mean concentrations of 474 \pm 184 ng Hg g⁻¹. This indicates that aspen trees were reallocating the Hg to new growth. Roots and soil of the Hg(0)-treated trees were also significantly higher than for control tree or MeHg exposures (Table 1), suggesting movement of the Hg through the vascular system to the roots and then secretion to the soil. Alternatively, the high soil Hg concentration could be attributed to dry deposition of Hg(0). However, Hg(0) is readily re-emitted with light and watering (Gustin et al., 2004; Briggs and Gustin, 2013), and this would remove Hg(0) deposited to the soil. Stem and branch concentrations were also higher than the controls by ~150 ng Hg g⁻¹ (p < 0.001). Since these were 1 y old trees, individual rings could not be analyzed. Senesced foliage from Hg(0) exposures had mean concentrations of 61 \pm 28 ng Hg g⁻¹ and was not significantly different from the MeHg exposures nor the control (p > 0.05), indicating resorption of Hg from aspen foliage.

3.1.2. Methylmercury

MeHg concentrations in control aspen foliage ranged from below the detection limit to 0.68 ng g⁻¹ (Table S1). For aspen that had been treated, concentrations measured were not different from control values except for a 0.89 and 1.7 ng g⁻¹ value that were associated with foliage from the Hg(0)

Table 1 Mean Hg concentrations (ng g $^{-1}$ dry weight \pm 1 σ , n=3–5 biological replicates) in aspen tissues pre-exposure, after exposures, and of senesced foliage for the fall immediately after the treatment. Concentrations without 1 σ are from n=1–2 biological replicates. "Bole (low)" means the 10 cm section at the base of the tree, and "Bole (high)" means the 10 cm section from 1 m above the base of the tree.

e (low) Bole (high) = 1 2 ± 0.3	Branches Buds
= 1 2 ± 0.3	3
2 ± 0.3	3
± 0.3 4 ± 1	7 ± 1 9
1 ± 21 157 ± 23	147 ± 47 330
± 0.4 4 ± 0.2	7 ± 2 8
0.3 3 ± 1	6 8
1 ± 3	
5 129 ± 109	
1 ± 3	
2 ± 3	
1	1 ± 21 157 ± 23 ± 0.4 4 ± 0.2 ± 0.3 3 ± 1 1 ± 3 129 ± 109

during exposure and the Pre-old foliage, and the Me¹⁹⁸Hg spike, respectively. Based on limited data, we observed that $\sim\!2$ % of the Hg in foliage was MeHg, similar to observations by others (Liu et al., 2021; Ericksen et al., 2003).

3.1.3. Foliar tissue component separation

For assimilation from Hg(0) exposure, 85 % of the Hg accumulated in the cell wall compared to the soluble and membrane fractions (Fig. 1, p < 0.001). The soluble and membrane fractions were not significantly different from each other. Relative levels of Hg(0) in the cell wall were, in order of decreasing values: Pre-new > Pre-old > During > Post >> Control. The high amounts of Hg found in tissues that only grew after a Hg exposure demonstrate that the Hg(0) assimilated during the spike was remobilized into new tissue. These results also indicate that Hg was preferentially associated with cell walls, regardless of whether it was assimilated directly from the air, or remobilized and transferred from another part of the tree.

It is not yet clear why Hg preferentially accumulates in cell walls of aspen leaves. The cell wall is made up of a diversity of polysaccharides, such a cellulose, hemicellulose, pectin, and lignins, as well as S containing proteins (i.e., containing cysteine and methionine residues). Because Hg often reacts with S compounds, we tested whether the relative abundance of Hg was proportional to the relative abundance of S in the different fractions. However, despite the wall having 85 % of the bound Hg, the relative amount of S was >17-times less than the soluble/membrane fraction. The concentration of S in the aspen foliage used here ranged from 49 to 251 μ g S g $^{-1}$ leaf material, while the amount of S that fractionated with the cell walls in each of 3 independent samples was below the assay's detection limit of 14.5 μ g S g $^{-1}$ leaf material. This indicates that the Hg is not simply partitioning to subcellular locations with the highest amounts of S. This is consistent with an analysis of Spanish moss in which hemicellulose in the cell was reported as a primary site for binding Hg (Sun et al., 2021).

To investigate how cell wall Hg-adducts could be remobilized during senescence and transported to new tissues, the manner in which potential changes in the redox environment might release cell wall-bound Hg was tested. During the preparation of cell wall fractions, the inclusion of 300 mM $\rm H_2O_2$ displaced nearly half of the bound Hg (51 \pm 14, 50 \pm 2, and 31 \pm 7 %, for pre-new, pre-old, and during, respectively, Table S2). While this $\rm H_2O_2$ -dependent displacement was less pronounced at 30 mM $\rm H_2O_2$, the effective concentration in this assay remains uncertain given that $\rm H_2O_2$ added to a crude plant extract has an expected half-life between 1 and 10 s (Akter et al., 2021). Although it is difficult to verify the magnitude of transient $\rm H_2O_2$ concentrations that actually occur in cell wall microenvironments during senescence, it is possible that much lower $\rm H_2O_2$

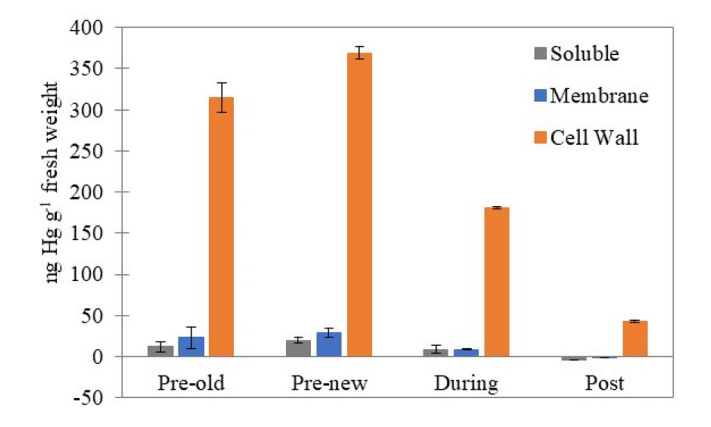


Fig. 1. Tissue fraction of aspen leaves indicate that Hg accumulates primarily in the cell wall fraction immediately following Hg(0) exposures as well as after remobilization to newly developed leaves. The relative abundance of Hg (ng g $^{-1}$ fresh weight of tissue) is shown for aspen foliage after fractionation into cell walls, membranes, and soluble components. Background control values were subtracted. Extractions were done using fresh tissue frozen with liquid nitrogen immediately after sample collection.

concentrations could also displace Hg-adducts in situations where smaller increases in H₂O₂ concentrations are continuously generated over periods of days, such as during plant senescence (Mhamdi and Van Breusegem, 2018). Importantly, the cell wall has a variety of redox systems that can produce different reactive oxygen species (ROS) or reactive nitrogen specific (RNS) (Del Río, 2015; Sobieszczuk-Nowicka, 2017; Dixon and Barros, 2019; Wang et al., 2019; Akter et al., 2021). While it is not yet clear how Hg-adducts are remobilized in aspen tissues, evidence here supports a model in which redox reactions driven by ROS or RNS could provide a non-enzymatic mechanism to release Hg for relocation. This remobilization could occur by directly reducing Hg(II) to Hg(0), or indirectly by breaking down cell wall structures and releasing small fragments containing Hg-adducts (Müller et al., 2009). It is also possible that some plants have a yet-to-be-identified enzymatic mechanism to breakdown organomercury compounds, analogous to the MerAB enzymes in bacteria and archaea that demethylate methylmecury (Christakis et al., 2021). During senescence, nutrients are mobilized (Mhamdi and Van Breusegem, 2018), and Hg could be transported to other tissues through the phloem in association with thiol containing proteins, iron-sulfur based proteins, amines, PO_4^{3-} , or carboxyl group compounds.

3.1.4. Hg isotope ratios

There was a small-magnitude, but significant, odd-MIF (Δ^{199} Hg = $0.20~\pm~0.02~\%$ (1 σ)) associated with the Hg(0) from the permeated trap that was used to treat the plants, and this was passed on to the Hg isotopic composition of the foliage with the same value within measurement uncertainty (Table S7). The average Δ^{199} Hg/ Δ^{201} Hg ratio was 1.68, which is consistent with nuclear volume fractionation (Ghosh et al., 2013), known to occur during evaporation of liquid Hg(0). The δ^{202} Hg value of -1.78 % for Hg from the permeated trap represents the magnitude of MDF associated with the gaseous Hg(0) before interaction with plant tissues, and serves as an initial value. The $\delta^{202}\text{Hg}$ value of -2.2 % for Hg from the inlet trap associated with the aspen Hg(0) chamber is evidence that this trapped Hg was subjected to additional MDF from the initial value, that is unrelated to Hg(0) interaction with aspen tissues. A small range of -3.82to -4.13~% in the $\delta^{202}\text{Hg}$ values of foliage tissues was observed and indicates a MDF of 2.04 to 2.35 % during oxidation and fixation of Hg in the foliage tissues. This is experimental confirmation of this fractionation, that has been observed in field studies of Hg isotope fractionation in foliage (Demers et al., 2013; Yu et al., 2016; Jiskra et al., 2019; Kurz et al., 2020; Douglas and Blum, 2019).

Hg spike isotopic measurements and isotope dilution calculations indicated 1.1 and 3.8 % (n = 2 trees) of the Hg in the roots was derived from the Me¹⁹⁸Hg that was added to the soil (Table S4). In general, the proportion of Hg from Me¹⁹⁸Hg found in foliage was low, ranging from 0.02 to 0.08 % of the HgT. For additional isotope data, see Tables S5-S8 and Fig. S1. For these samples, the ability of the isotope dilution calculation to resolve sample-to-sample differences in Me¹⁹⁸Hg content was limited when the proportion of Me¹⁹⁸Hg was lower than 0.1 % of HgT. This reduction in resolving power is partly attributable to limited availability of sample material and low HgT content that contributed to greater measurement uncertainty. Nevertheless, the even-MIF isotope results for these samples clearly indicate that Hg from the Me¹⁹⁸Hg spike is present in the leaf material. Values of Δ^{200} Hg determined for leaves from the Me¹⁹⁸Hg treatment range from -0.21 to -0.87 % and are 3 to 40 times larger than the 2σ uncertainty determined for the analyses (Tables S3 and S8). In contrast, Δ^{200} Hg of average Western US TGM (Kurz et al., 2020), which is similar to that found for leaves exposed to natural isotope abundance Hg, is only -0.09 ‰. Moreover, Fig. S1 illustrates that Δ^{200} Hg and Δ^{204} Hg values determined for samples from the Me¹⁹⁸Hg treatment plot along a trend that is very nearly coincident with the trend defined by mixing of NIST SRM3133 (no even-MIF) and the Me¹⁹⁸Hg spike. Root to leaf translocation of Hg derived from the Me198Hg spike is one explanation for the observed foliar even-MIF isotope composition. Another possible explanation is reduction of Me¹⁹⁸Hg in the soil and emission of spike-Hg as Hg(0) that retains the spike's even-MIF signature, which then mixes with ambient Hg(0) and becomes available to the leaves via direct uptake from the atmosphere. However, the latter explanation is likely not the cause for the observation of ¹⁹⁸Hg in the foliage, for spikes were added well below the soil surface.

3.2. Austrian pine

Pine trees were spiked simultaneously with Me¹⁹⁸Hg and Hg(0). MeHg was detected in the Pre-new and Pre-old control foliage. For the trees treated with Me¹⁹⁸Hg and Hg(0), MeHg was measured in the roots of one sample (0.9 ng g $^{-1}$), in the Pre-new bole of both samples (0.16 and 0.19 ng g $^{-1}$), and in the Pre-old and Pre-new foliage of one sample (1.57 and 0.47 ng g $^{-1}$, respectively); tissues from 2 biological replicates were analyzed for MeHg concentrations. These concentrations were similar to those for the Pre-old and Pre-new needles for one control tree (0.98 and 0.71 ng g $^{-1}$, respectively) (Table S1). Because this species did not mobilize Hg after exposure (discussed below), Hg isotope ratios were not analyzed.

Soil and root Hg concentrations increased after the spike additions (Fig. 2). Soil Hg concentrations increased in autumn when the trees were placed outside, and the soil at that location was mixed with the potting soil, increasing Hg concentrations. Root concentrations were variable (Fig. 2).

Concentrations in the bole were not affected by the Hg(0) nor $Me^{198}Hg$ spike addition. Bole Hg concentrations decreased over time in the treated and control trees, likely due to growth dilution. Hg concentrations increased in the Pre-old and Pre-new foliage after the treatment. Autumnand spring-sampled needle Hg concentrations were significantly lower than that observed after the treatment. No Pre-new needles grew during the exposure and the Post needles in spring of 2021 had low Hg concentrations (2.8 ng g^{-1}).

These data indicate that Austrian pine trees assimilated Hg(0) when exposed, but did not subsequently translocate it to other tissues, and the Preold and Pre-new needle concentrations decreased over time. Again, a small amount (0.16 and 0.19 ng g $^{-1}$) of the $^{198}{\rm Hg}$ spike (17 \pm 1 ng) added to the soil was moved into the bole. The decrease in foliage concentrations could be due to off gassing from the leaf interior. Yuan et al. (2019) found, using Hg isotopes associated with evergreen beech trees, that after foliage assimilated Hg(0), leaves became progressively enriched in lighter isotopes and depleted in odd-mass isotopes. This shift was caused by emission of metabolized Hg in the leaf interior and release as Hg(0) from the foliage.

Peckham et al. (2019a, 2019b) hypothesized that resorption of Hg from the foliage was occurring due to a decrease in concentrations associated with old foliage from fall to spring, similar to that observed here. However,

new foliage concentrations in the spring were not significantly different than the control suggesting that Austrian pine foliage were not reallocating Hg. It is likely Hg reduction and loss was occurring as suggested by Yuan et al. (2019).

4. Implications

This study and others have demonstrated that different tree species take up Hg via the foliage, but the fate of assimilated Hg has not been fully explored. Aspen trees resorbed Hg during senescence and translocated Hg to different tissues during growth. This suggests aspen are not good recorders of atmospheric Hg concentrations using tree rings, which is consistent with evidence from field studies (Gustin et al., 2022; Siwik et al., 2009). In contrast, the 3 y old Austrian pine trees, used in this study, did not remobilize and redistribute Hg between tree tissues, consistent with evidence from Peckham et al. (2019a, 2019b).

Aspen is a deciduous tree that loses its leaves in the fall and resorbs nutrients from the leaves to the bole and branches, while pine species lose needles gradually over the year and nutrients in old needles are moved into new needles (Yuan et al., 2018). Deciduous trees resorb more nutrients than conifer species (Brant and Chen, 2015). The behavior of these tree species may not necessarily be generalized to other tree species. For example, several studies have shown that radial translocation occurs in different pine species (Arnold et al., 2018; Chellman et al., 2020; Novakova et al., 2021). More work needs to be done to understand the potential for radial translocation in tree species being used for tree-ring studies.

Aspen foliage component analyses demonstrated that Hg was primarily concentrated in the cell wall. The displacement of Hg from the cell wall by redox active molecules, such as $\rm H_2O_2$, suggests a potential non-enzymatic mechanism by which Hg could be remobilized during senescence. Finally, experiments verified that light Hg isotopes were preferentially oxidized within foliage leading to a MDF between Hg(0) and Hg(II) in foliage of 2.04 to 2.35 ‰, similar to that observed in field studies. MeHg concentrations measured in foliage were not statistically different from the control and a small amount of the $\rm Me^{198}Hg$ spike was found in aspen foliage, indicating that organic Hg can be transferred from the soil to foliage, supporting the work of Tabatchnick et al. (2012) who suggested in vivo MeHg production.

Data availability

All raw data are available from the corresponding author upon request.

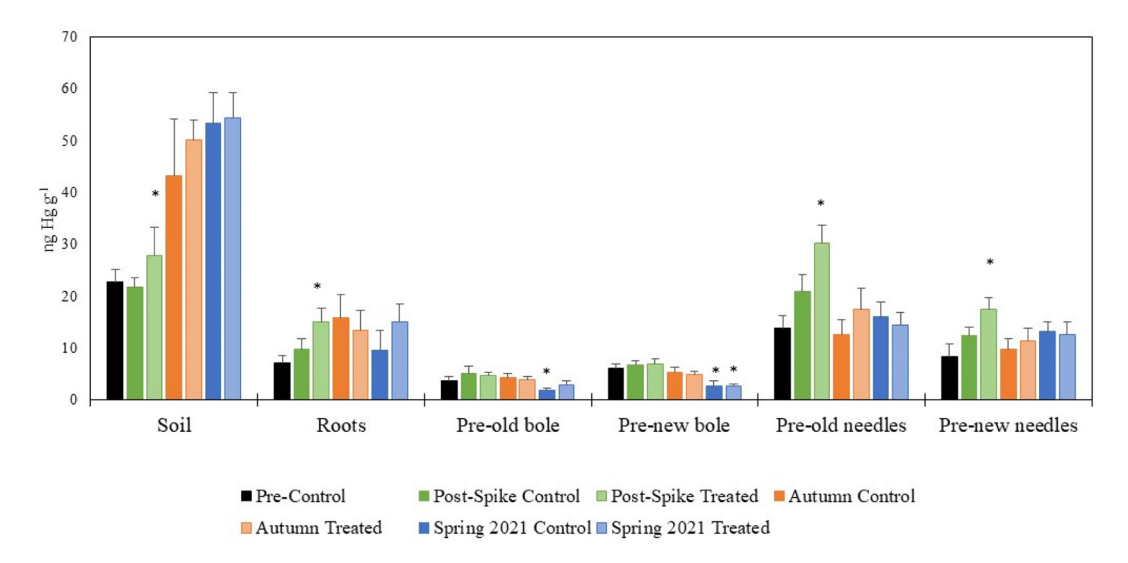


Fig. 2. Distribution of Hg (ng g^{-1}) in Austrian pine tissues as a function of season for plants treated with Hg(0) via the air and Me¹⁹⁸Hg spikes to the soil. Asterisks indicate where concentrations were significantly greater than the control.

CRediT authorship contribution statement

Mae Gustin helped with experimental design, compiled the data into figures and tables, and wrote the paper. Sarrah Dunham-Cheatham helped with the experimental design, collected and analyzed samples, oversaw others helping with sampling and analysis. She compiled the data into tables and helped write the manuscript. Jeff Harper and Won-Gyu Choi developed the methods for separating cell components and doing the $\rm H_2O_2$ experiments, and helped with writing of the paper. Joel Blum and Marcus Johnson were responsible for the isotope analyses and wrote the isotope components of the paper, and helped with writing the manuscript.

Data availability

Data will be made available on request.

Declaration of competing interest

The authors declare no conflict of interest.

Acknowledgments

This work was funded by USDA HATCH grant. The authors would like to thank: Ben Ingle for his support with monitoring and watering the trees, as well as assisting with conducting the experiments; and Nicole Choma, Cameron French, Su-Hwa Kim, Samantha Leftwich, Livia Lown, Adriel Luippold, Jong Chan Park, Margarita Vargas Estrada, and Josh Vernaz, for their help with various stages of the project; Emily Medina for preparing the foliage component samples; Elizabeth Brown for her help with trouble-shooting pests and repotting the aspen trees; and Scott Huber for his help planting trees outside for overwintering. We thank Professor Peter Weisberg for reading over a version of this manuscript and 3 anonymous reviewers for providing thoughtful comments.

Appendix A. Supplementary data

Supplementary data to this article can be found online at https://doi.org/10.1016/j.scitotenv.2022.158101.

References

- Akter, S., Khan, M.S., Smith, E.N., Flashman, E., 2021. Measuring ROS and redox markers in plant cells. RSC Chem. Biol. 2 (5), 1384–1401. https://doi.org/10.1039/d1cb00071c PMID: 34704044; PMCID: PMC8495998.
- Arnold, J., Gustin, M.S., Weisberg, P.J., 2018. Evidence for nonstomatal uptake of Hg by aspen and translocation of Hg from foliage to tree rings in Austrian pine. Environ. Sci. Technol. 52 (3), 1174–1182.
- Biswas, A., Blum, J.D., Keeler, G.J., 2008. Mercury storage in surface soils in a central Washington forest and estimated release during the 2001 Rex Creek Fire. Sci. Total Environ. 404 (1), 129–138. https://doi.org/10.1016/j.scitotenv.2008.05.
- Blum, J.D., Sherman, L.S., Johnson, M.W., 2014. Mercury isotopes in earth and environmental sciences. Annu. Rev. Earth Planet. Sci. 42, 249–269.
- Brant, A.N., Chen, H.Y.H., 2015. Patterns and mechanisms of nutrient resorption in plants. Crit. Rev. Plant Sci. 34, 471–486.
- Briggs, C., Gustin, M.S., 2013. Building upon the conceptual model for soil mercury flux: evidence of a link between moisture evaporation and Hg evasion. Water Air Soil Pollut. 224, 1744. https://doi.org/10.1007/s11270-013-1744-5 September 2013.
- Carrasco-Gil, S., Siebner, H., LeDuc, D.L., Webb, S.M., Millan, R., Andrews, J.C., Hernandez, L.E., 2013. Mercury localization and speciation in plants grown hydroponically or in a natural environment. Environ. Sci. Technol. 47 (7), 3082–3090.
- Chellman, N., Csank, A., Gustin, M.S., Arienzo, M.M., Estrada, M.V., McConnell, J.R., 2020.
 Comparison of co-located ice-core and tree-ring mercury records indicates potential radial translocation of mercury in whitebark pine. Sci. Total Environ. 743.
- Christakis, C.A., Barkay, T., Boyd, E.S., 2021. Expanded diversity and phylogeny of mer genes broadens mercury resistance paradigms and reveals an origin for MerA among thermophilic archaea. Jun 23Front. Microbiol. 12, 682605. https://doi.org/10.3389/fmicb. 2021.682605 PMID: 34248899; PMCID: PMC8261052.
- Del Río, L.A., 2015y. ROS and RNS in plant physiology: an overview. J. Exp. Bot. 66 (10), 2827–2837. https://doi.org/10.1093/jxb/erv099 Epub 2015 Apr 7 PMID: 25873662.

- Demers, J.D., Blum, J.D., Zak, D.R., 2013. Mercury isotopes in a forested ecosystem: implications for air-surface exchange dynamics and the global mercury cycle. Glob. Biogeochem. Cycles 27 (1), 222–238.
- Dennis, K.K., Uppal, K., Liu, K.H., Ma, C.Y., Liang, B., Go, Y.M., Jones, D., 2019. Phytochelatin database: a resource for phytochelatin complexes of nutritional and environmental metals. Database: J. Biol. Databases Curation 2019.
- Dixon, R.A., Barros, J., 2019. Lignin biosynthesis: old roads revisited and new roads explored.

 DecOpen Biol. 9 (12), 190215. https://doi.org/10.1098/rsob.190215 Epub 2019 Dec 4.

 PMID: 31795915; PMCID: PMC6936255.
- Douglas, T.A., Blum, J.D., 2019. Mercury isotopes reveal atmospheric gaseous mercury deposition directly to the Arctic coastal snowpack. Environ. Sci. Technol. Lett. 6 (4), 235–242. https://doi.org/10.1021/acs.estlett.9b00131.
- Du, S.H., Fang, S.C., 1983. Catalase activity of C3 and C4 species and its relationship to mercury-vapor uptake. Environ. Exp. Bot. 23 (4), 347–353.
- Ericksen, J.A., Gustin, M.S., 2004. Foliar exchange of mercury as a function of soil and air mercury concentrations. Sci. Total Environ. 324 (1–3), 271–279.
- Ericksen, J.A., Gustin, M.S., Schorran, D.E., Johnson, D.W., Lindberg, S.E., Coleman, J.S., 2003. Accumulation of atmospheric mercury in forest foliage. Atmos. Environ. 37 (12), 1613–1622.
- Ghosh, S., Schauble, E.A., Couloume, G.L., Blum, J.D., Bergquist, B.A., 2013. Estimation of nuclear volume dependent fractionation of mercury isotopes in equilibrium liquid-vapor evaporation experiments. Chem. Geol. 336, 5–12.
- Gustin, M.S., Ericksen, J.A., Schorran, D.E., Johnson, D.W., Lindberg, S.E., Coleman, J.S., 2004. Application of controlled mesocosm for understanding mercury plant-soil-air exchange. Environ. Sci. Technol. 38, 6044–6050.
- Gustin, M.S., Ingle, B., Dunham-Cheatham, S.M., 2022. Further investigations into the use of tree rings as archives of atmospheric mercury concentrations. Biogeochemistry, 93
- Iverfeldt, A., 1991. Mercury in forest canopy throughfall water and its relation to atmospheric deposition. Water Air Soil Pollut. 56 (1), 553–564.
- Jiskra, M., Sonke, J.E., Agnan, Y., Helmig, D., Obrist, D., 2019. Insights from mercury stable isotopes on terrestrial-atmosphere exchange of Hg(0) in the Arctic tundra. Biogeosciences 16 (20), 4051–4064. https://doi.org/10.5194/bg-16-4051-2019.
- Kurz, A.Y., Blum, J.D., Gratz, L.E., Jaffe, D.A., 2020. Contrasting controls on the diel isotopic variation of Hg-0 at two high elevation sites in the Western United States. Environ.Sci. Technol. 54 (17), 10502–10513. https://doi.org/10.1021/acs.est.0c01918.
- Liu, Y., Liu, G., Wang, Z., Guo, Y., Yin, Y., Zhang, X., Cai, Y., Jiang, G., 2021. Understanding foliar accumulation of atmospheric Hg in terrestrial vegetation: progress and challenges. Crit. Rev. Environ. Sci. Technol. 1–22.
- Manceau, A., Bustamante, P., Haouz, A., Bourdineaud, J.P., Gonzalez-Rey, M., Lemouchi, C., Gautier-Luneau, I., Geertsen, V., Barruet, E., Rovezzi, M., Glatzel, P., Pin, S., 2019. Mercury(II) binding to metallothionein in Mytilus edulis revealed by high energy-resolution XANES spectroscopy. Chem. Eur. J. 25 (4), 997–1009.
- Mhamdi, A., Van Breusegem, F., 2018. Reactive oxygen species in plant development. Development 145 (15), dev164376. https://doi.org/10.1242/dev.164376 1 August.
- Millhollen, A.G., Gustin, M.S., Obrist, D., 2006. Foliar mercury accumulation and exchange for three tree species. Environ. Sci. Technol. 40 (19), 6001–6006.
- Müller, K., Linkies, A., Vreeburg, R.A., Fry, S.C., Krieger-Liszkay, A., Leubner-Metzger, G., 2009. In vivo cell wall loosening by hydroxyl radicals during cress seed germination and elongation growth. AugPlant Physiol. 150 (4), 1855–1865. https://doi.org/10.1104/pp.109.139204 Epub 2009 Jun 3. PMID: 19493972; PMCID: PMC2719145.
- Munthe, J., Hultberg, H., Iverfeldt, Å., 1995. Mechanisms of deposition of methylmercury and mercury to coniferous forests. Water Air Soil Poll. 80, 363–371.
- Novakova, T., Navratil, T., Demers, J.D., Roll, M., Rohovec, J., 2021. Contrasting tree ring hg records in two conifer species: multi-site evidence of species-specific radial translocation effects in scots pine versus European larch. Sci. Total Environ. 762.
- Peckham, M.A., Gustin, M.S., Weisberg, P.J., Weiss-Penzias, P., 2019a. Results of a controlled field experiment to assess the use of tree tissue concentrations as bioindicators of air Hg. Biogeochemistry 142 (2), 265–279.
- Peckham, Matthew A., Gustin, Mae Sexauer, Weisberg, Peter J., 2019b. Assessment of the suitability of tree rings as archives of global and regional atmospheric mercury pollution. Environ. Sci. Technol. https://doi.org/10.1021/acs.est.8b06786.
- Siwik, E.I.H., Campbell, L.M., Mierle, G., 2009. Fine-scale mercury trends in temperate deciduous tree leaves from Ontario, Canada. Sci. Total Environ. 407 (24),
- Sobieszczuk-Nowicka, E., 2017. Polyamine catabolism adds fuel to leaf senescence. JanAmino Acids 49 (1), 49–56. https://doi.org/10.1007/s00726-016-2377-y Epub 2016 Dec 30. PMID: 28039518; PMCID: PMC5241338.
- Stamenkovic, J., Gustin, M.S., 2009. Nonstomatal versus stomatal uptake of atmospheric mercury. Environ. Sci. Technol. 43 (5), 1367–1372.
- Sun, X., Li, P., Zheng, G., 2021. Cellular and subcellular distribution and factors influencing the accumulation of atmospheric Hg in Tillandsia usneoides leaves. J. Hazard. Mater. (ISSN: 0304-3894) 414, 125529. https://doi.org/10.1016/j. jhazmat.2021.125529.
- Tabatchnick, M.D., Nogaro, G., Hammerschmidt, C.R., 2012. Potential sources of methylmercury in tree foliage. Environ. Pollut. 160, 82–87.
- Tehrani, H.S., Moosavi-Movahedi, A.A., 2018. Catalase and its mysteries. Prog. Biophys. Mol. Biol. 140, 5–12.
- Vainshtein, B.K., Melikadamyan, W.R., Barynin, V.V., Vagin, A.A., Grebenko, A.I., 1981. Three-dimensional structure of the enzyme catalase. Nature 293 (5831), 411–412.
- Wang, W., Paschalidis, K., Feng, J.C., Song, J., Liu, J.H., 2019. Polyamine catabolism in plants: a universal process with diverse functions. May 7. Front. Plant Sci. 10, 561. https://doi.org/10.3389/fpls.2019.00561 PMID: 31134113; PMCID: PMC6513885.

- Wang, X., Yuan, W., Lin, C.J., Wu, F., Feng, X.B., 2021. Stable mercury isotopes stored in Masson Pinus tree rings as atmospheric mercury archives. J. Hazard. Mater. 415, 125678.
 Yu, B., Fu, X.W., Yin, R.S., Zhang, H., Wang, X., Lin, C.J., Wu, C.S., Zhang, Y.P., He, N.N., Fu, P.Q., et al., 2016. Isotopic composition of atmospheric mercury in China: new evidence for sources and transformation processes in air and in vegetation. Environ. Sci. Technol. 50 (17), 9262–9269. https://doi.org/10.1021/acs.est.6b01782.
- Yuan, Z.Y., Shi, X.R., Jiao, F., Han, F.P., 2018. N and P resorption as functions of the needle age class in two conifer trees. J. Plant Ecol. 11, 780–788.
- Yuan, W., Sommar, J., Lin, C.J., Wang, X., Li, K., Liu, Y., Zhang, H., Lu, Z., Wu, C., Feng, X., 2019. Stable isotope evidence shows re-emission of elemental mercury vapor occurring after reductive loss from foliage. Environ. Sci. Technol. 53 (2), 651–660.